

Experimental Study of Continuous Wave Hydrogen-Fluoride Chemical Laser Overtone Performance

D. L. Carroll,* L. H. Sentman,† P. T. Theodoropoulos,* R. E. Waldo,* and S. J. Gordon*
University of Illinois at Urbana-Champaign, Urbana, Illinois 61801

The overtone lasing performance of the supersonic continuous wave hydrogen-fluoride chemical laser at the University of Illinois at Urbana-Champaign was optimized by the same set of flow rates that optimized the fundamental performance. When the absorption/scattering losses of the mirrors were taken into account, an overtone efficiency (the ratio of overtone power to maximum fundamental power for the same flow conditions) of 70–90% was achieved. The overtone efficiency was a strong function of medium saturation. There was no significant change in overtone power and efficiency as the mode volume increased. However, there was an increase in the number of lasing lines and a shift to higher rotational (J) lines. Overtone performance was as sensitive to cavity pressure as fundamental performance was. There was no significant change in overtone efficiency when the method of helium injection was changed.

I. Introduction

ONE of the basic issues associated with the development of high-energy lasers is scaling to required brightness levels (the ratio of laser power times exit aperture diameter to the square of the wavelength of the laser, i.e., $B=PA/\lambda^2$). The hydrogen-fluoride (HF) overtone laser is of interest because it would use existing HF fundamental laser technology at the overtone wavelengths (approximately half the wavelength of the fundamental transitions), which would significantly increase the brightness of the laser system if the overtone power is a significant fraction of the fundamental power. Initial studies of the HF overtone ($a\ 2\rightarrow 0$, $\Delta v=2$ vibrational transitions, $\lambda=1.3\text{--}1.4\ \mu\text{m}$) laser have identified a number of issues that affect the scalability of this device.^{1–6} These include the fraction of the fundamental ($2\rightarrow 1$ and $1\rightarrow 0$, $\Delta v=1$ vibrational transitions $\lambda=2.5\text{--}3.1\ \mu\text{m}$) power that is obtainable in the overtone, the magnitude of the residual fundamental gain while lasing on the overtone, relative sizes of overtone and fundamental mode widths, relation of fundamental and overtone zero power gain distributions to power spectral distributions, and the effect of rotational relaxation on power extraction, among others.

To investigate these issues, the overtone performance of the supersonic laser at the University of Illinois at Urbana-Champaign (UIUC) was characterized as a function of flow rates, cavity pressure, mode volume, mirror reflectivity, and method of helium (He) injection. The supersonic laser fundamental performance data are presented in Sec. II, and the overtone performance data are presented in Sec. III. In Sec. IV, the fundamental and overtone data are compared to obtain overtone efficiencies. Several concluding remarks are given in Sec. V.

II. Supersonic Laser Fundamental Performance

The overtone experiments were performed on the low-pressure, cw, arc-driven supersonic HF chemical laser⁷ that was designed and constructed at UIUC. Supersonic slit nozzles for the primary (fluorine plus other molecules) and secondary (hydrogen) nozzles were chosen to provide a two-dimensional flowfield to simplify the calculation of the fluid dynamic mixing. The laser is described

briefly in Sec. II.A and in more detail in Ref. 7. Two methods of He injection were investigated. In the first method, He was injected through the anodes of the discharge tubes along with sulfur-hexafluoride (SF_6) and oxygen (O_2). In the second method, He was injected through a concentric sonic slit at the exit of the discharge tubes, after the SF_6 had been dissociated by the high voltage arc. The first method is denoted as regular He injection and the second is denoted as concentric sonic slit (CSS) He injection.

A. Experimental Layout and Procedure

The experimental layout is illustrated in Fig. 1a. The parallel slit nozzles, Fig. 1b, which are 5 mm high, exhaust into the center of a channel that is 1.5 cm high, thus forming a freejet. The width of the nozzle bank is 30 cm. The fluorine (F) atoms and hydrogen (H_2) molecules are injected through alternating parallel slit nozzles, Fig. 1b. These gases mix diffusively, creating a flame sheet containing excited HF molecules in the laser cavity. The exit Mach number is approximately 2.0 for the primary nozzles and approximately 0.66 for the secondary nozzles; the pressure at the exit of all of the nozzles is matched at approximately 2.2 Torr. The mirrors were separated by a distance of 1 m. The optical cavity was mounted on translation stages in vacuum boxes that were attached to the laser body. Vacuum boxes were used to eliminate the significant loss mechanism caused by intracavity Brewster windows. By moving the translation stages, the optical axis location X_c for peak power was measured. It was necessary to design water-cooled mirror mounts to effectively dissipate power absorbed by the mirrors inside the vacuum boxes.

The total multiline power was measured by placing a Scientech Model 362 power meter into each of the two outcoupled beams, Fig. 1a. For any tests that were likely to exceed a power of 10 W, the power of the beam was reduced 90% by a chopper to prevent damage to the power meter. The measured single-pass transmission loss of the calcium-fluoride (CaF_2) windows was 4.5%, independent of wavelength. All reported powers are corrected for the CaF_2 window loss.

The flow rates that optimized fundamental performance using regular He injection were 0.0425 g/s of He, 0.135 g/s of O_2 , 1.54 g/s of SF_6 , and 0.0535 g/s of H_2 . The flow rates that optimized fundamental performance using CSS He injection were 0.097 g/s of He, 0.135 g/s of O_2 , 0.825 g/s of SF_6 , and 0.0415 g/s of H_2 . For both methods of He injection, the He purge flow rates that optimized performance were 0.0125 g/s in the base purge at the center of the nozzle bank and 0.0125 g/s to the He purge ducts, Fig. 1.

The pressures in the laser cavity and upstream of the nozzle bank were measured by two Baratron pressure gauges that were connected to static pressure taps upstream and downstream of the

Received Jan. 31, 1992; revision received Aug. 3, 1992; accepted for publication Aug. 4, 1992. Copyright © 1992 by the American Institute of Aeronautics and Astronautics, Inc. All rights reserved.

*Research Assistant, Aeronautical and Astronautical Engineering Department; currently, Postdoctoral Research Associate. Member AIAA.

†Professor, Aeronautical and Astronautical Engineering Department. Associate Fellow AIAA.

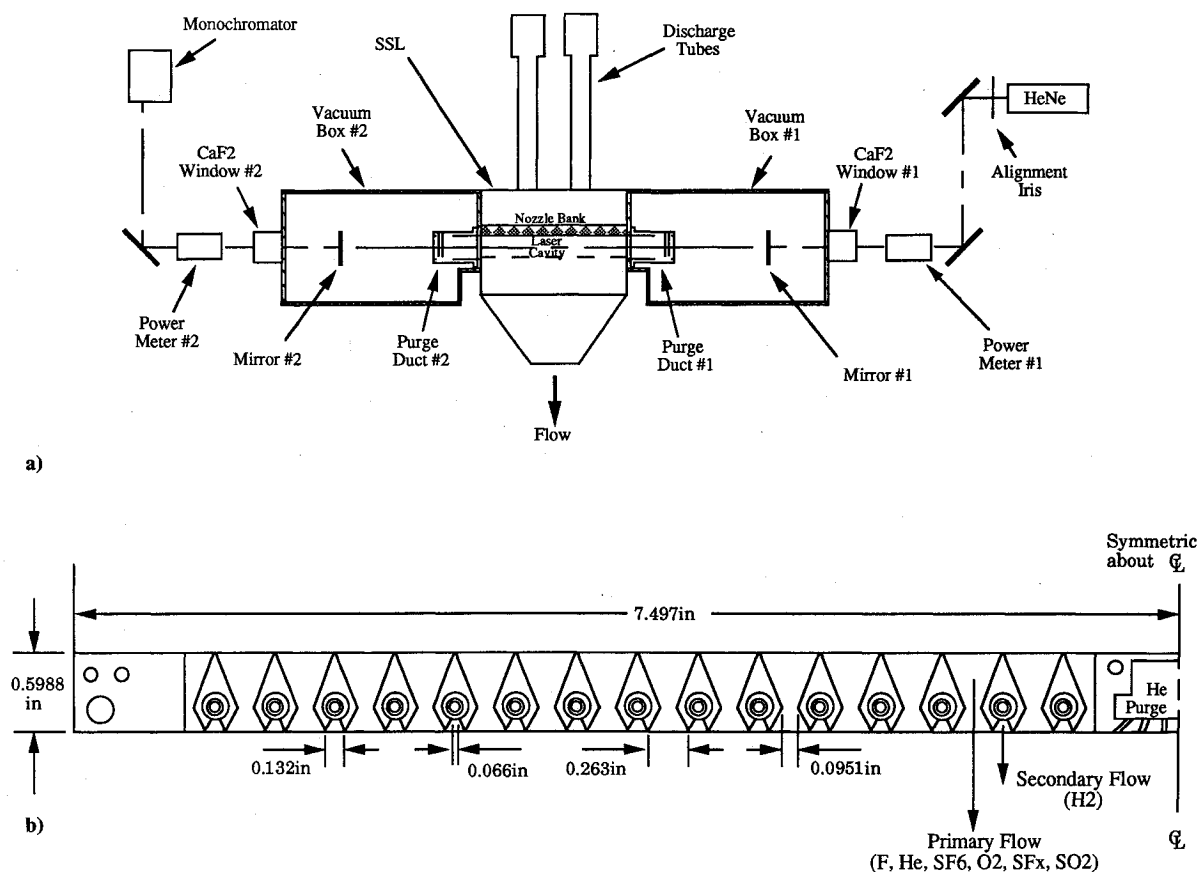


Fig. 1 a) Layout of the UIUC supersonic laser fundamental and overtone experiments, and b) enlarged schematic of half of the nozzle bank.

nozzle bank. Because the downstream pressure was measured 39 mm downstream from the nozzle exit plane (NEP) at the top of the laser cavity (5 mm above the freejet), the reported pressures do not accurately represent those in the lasing zone (which extends approximately 12 mm from the NEP). The pressure in the laser cavity (downstream from the nozzle bank) was adjusted by a flow control valve. The flow control valve was completely opened for the lowest cavity pressures of 5.1 and 4.4 Torr for regular and CSS He injection, respectively. The flow control valve was partially closed to achieve higher cavity pressures. The pressures upstream of the nozzle bank were 17.8 and 12.4 Torr for regular and CSS He injection, respectively. The upstream pressure was unaffected when the flow control valve was partially closed to obtain higher cavity pressures. This was experimental confirmation that the primary nozzles were choked.

A Rofin (now Monolight) RSO 6000 series scanning monochromator was used to measure the spectral content of the laser beam. A 0.25-mm diameter pinhole was placed in front of the 0.2-mm entrance slit to provide spatial resolution and decrease the power incident on the detector. The monochromator and detector were mounted on horizontal and vertical translation stages, which were attached to the optical bench. This allowed two-axis translation with the ability to scan across the intensity profile of the outcoupled laser beam. The signal from the monochromator was averaged over 100 consecutive digitizations using a Tektronix 7854 digitizing oscilloscope. The Tektronix MP2501 data acquisition system consisting of the 7854 oscilloscope, a 4041 computer, a 4105 display terminal, a P6202A FET probe, and a 4695 graphics printer was used to acquire, store, and plot the observed power spectral distributions.

A piece of graph paper was used to measure the beam size observed on a thermal image plate. This method agreed well with more precise beam size measurements made by scanning across the center of the beam vertically and horizontally with the monochromator.

B. Fundamental Performance

Since one of the main issues of overtone laser development is the fraction of the fundamental power that can be obtained in the overtone, the fundamental performance of the supersonic laser (SSL) is summarized first. The mirrors used for the fundamental measurements were 2-m radius of curvature concave mirrors with a 1-m separation.

For the purposes of computing overtone efficiencies, the most important fundamental data are the maximum fundamental powers for different flow conditions. The fundamental stable resonator performance data as a function of outcoupler reflectivity, method of He injection, and cavity pressure are presented in detail in Ref. 8. The highest fundamental power observed with regular He injection at 5.1 Torr was 63.0 W with a 93% reflective outcoupler. Modeling calculations have shown that about 10% of the outcoupled fundamental power may be lost to absorption/scattering when using high reflectivity outcouplers. With this correction, the maximum power is estimated as 69.3 W. During the measurement of the zero power gain in the SSL, it was found that there was significant absorption of the $P_1(4-6)$ and $P_2(4,5)$ lines due to SF_x (fragments of SF_6 from the discharge arcs) species.^{7,9} When this absorption was included in the modeling studies of the SSL, better agreement between predicted and measured spectra and power was obtained. The inclusion of the SF_x absorption in modeling calculations decreased the power by approximately 10%. If the measured power is corrected for this loss, the maximum power is estimated as 76.2 W. Thus, the maximum fundamental power for regular He injection at 5.1 Torr is 63.0–76.2 W. The beam size at maximum power was approximately 5.5 mm high by 10.0 mm wide.

The highest observed power with CSS injection at 4.4 Torr was 58.5 W with a 96% reflective outcoupler and at 4.8 Torr was 51.7 W with a 93% outcoupler. If a 10% absorption/scattering loss when using high reflectivity outcouplers and a 10% SF_x absorption loss are included, the maximum power is estimated as 70.8 W at 4.4 Torr and 62.6 W at 4.8 Torr. Thus, the maximum fundamental

power for CSS He injection at 4.4 Torr is 58.5–70.8 W and at 4.8 Torr is 51.7–62.6 W. The beam size at maximum power was approximately 6.0 mm high by 11.5 mm wide, independent of pressure.

III. Supersonic Laser Overtone Performance

The flow rates that optimized the fundamental regular He injection performance optimized the overtone regular He injection performance. This was also true for the nozzle bank and vacuum box purge duct He purge flow rates. The overtone mirrors are opaque to visible wavelengths, which made it impossible to correctly align the front surfaces of both overtone mirrors with the HeNe alignment laser, i.e., only one of the two overtone mirrors could have its front surface aligned with the HeNe laser. Hence, it was often necessary to adjust the alignment of this mirror just to obtain overtone lasing, and therefore it was not possible to obtain reproducible measurements of X_c for peak power by translating the optical cavity. A better estimate was obtained by assuming that the upstream edge of the output beam was at the nozzle exit plane and dividing the size of the mode measured on a thermal image plate by two.

In all of the experiments reported here, the overtone mirrors were placed 1 m apart. The mirrors were nominally 99.7% reflective over the range of 1.3–1.4 μm and less than 1% reflective over the range 2.5–3.1 μm . The substrates were silicon that was transparent to the fundamental wavelengths. Data were obtained for three sets of 4-m radii of curvature (hereafter abbreviated as 4mCC), one set of 8-m and 30-m radii of curvature, one set of flat mirrors, and one set of nominal 98% reflective 4mCC mirrors.

Early experiments showed that it was vital to clean the overtone mirrors before every test run. The overtone mirrors were cleaned with lens paper and a mixture of 75% 1,1,1-trichloroethane and 25% ethanol having a nonvolatile residue of less than 1 ppm.¹⁰ The front surface of each mirror was cleaned twice and the back surface once before every run. Cleaning the front surface only once was often found to be insufficient (low overtone powers observed), whereas more than two cleanings did not improve overtone performance.

A. Reflectivity and Transmissivity of the Overtone Mirrors

Since the overtone is a low gain system that requires high-reflectivity mirrors to lase, small scattering/absorption losses have a large effect on the outcoupled power. To obtain an accurate estimate of the overtone efficiency of the SSL, the reflectivity and transmissivity of the nominally 99.7% reflective nos. 1 and 2 4mCC mirrors were measured by Helios. These reflectivity measurements verified that the nominally 99.7% reflective overtone optics were indeed approximately 99.7%, and therefore all of the

Rocky Mountain Instruments (RMI) overtone mirrors were assumed to have the specified reflectivity, with the exception of the two mirrors measured by Helios. The overtone transmission measurements for the 4mCC nos. 1 and 2 mirrors agreed well with Helios' overtone transmission measurements; thus, the UIUC transmission measurements were used for all of the overtone mirrors. The inferred absorption/scattering loss was calculated from the assumption that the reflectivity plus transmissivity plus absorption/scattering should equal one (Table 1). These data were used to calculate the overtone efficiency; see Sec. IV.

B. Overtone Performance

Table 2 summarizes the SSL overtone performance for several combinations of the overtone mirrors. Except for the nos. 5 and 6 concave 4mCC mirrors, the data were quite reproducible and insensitive to the radii of curvature of the mirrors. The data for the nos. 5 and 6 4mCC mirrors showed an immediate degradation of the coatings of these mirrors. These data for these mirrors were taken over about a week. They now consistently give 13–14 W of overtone power. The nos. 1 and 2 4mCC mirrors were used exten-

Table 1 Assumed reflectivity and measured transmissivity measurements used to obtain the inferred absorption plus scattering losses for various overtone mirrors

Mirror ^a	Assumed reflectance, %	Measured transmittance, %	Inferred A+S, %
4mCC 1-bd	99.78	0.064	0.156
4mCC 1-ad	99.68	0.064	0.256
4mCC 2	99.67	0.067	0.263
4mCC 3	99.70	0.073	0.227
4mCC 4	99.70	0.080	0.220
4mCC 5-bd	99.75	0.081	0.169
4mCC 6-bd	99.75	0.074	0.176
4mCC 5-ad	99.70	0.081	0.219
4mCC 6-ad	99.70	0.074	0.226
4mCC 7	98.00	1.130	0.870
4mCC 8	98.00	1.087	0.139
8mCC 1	99.70	0.084	0.216
8mCC 2	99.70	0.080	0.220
30mCC 1	99.70	0.084	0.216
30mCC 2	99.70	0.078	0.222
Flat 1	99.70	0.063	0.237
Flat 2	99.70	0.071	0.229
Flat 3	99.70	0.071	0.229
Flat 4	99.70	0.129	0.171

^abd—before degradation, ad—after degradation.

Table 2 Supersonic laser, regular He injection, overtone outcoupled power, and beam size data as a function of mode volume and medium saturation at 5.1 Torr; all of the mirrors are nominally 99.7% reflective except for the 4mCC nos. 7 and 8 mirrors, which are 98% reflective

Mirror no. 1 ^a	Mirror no. 2 ^a	Mirror no. 1		Mirror no. 2		Total power, W	Spectral lines lasing
		Power, W	Beam size, mm ²	Power, W	Beam size, mm ²		
Mode volume							
4mCC 1-bd	4mCC 2	5.63	4×6	5.90	4×6	11.5	$P_{20}(8-11)$
4mCC 1 -bd	Flat 2	6.27	5×8	5.78	3×5	12.1	$P_{20}(7-11)$
8mCC 1	8mCC 2	6.51	5×7	5.38	5×7	11.9	$P_{20}(8-11)$
30mCC 1	30mCC 2	6.37	5×6.5	6.05	4.5×6.5	12.4	$P_{20}(8-12)$
30mCC 2	Flat 2	6.27	5×7	6.27	3×7	12.5	$P_{20}(7-12)$
Flat 2	Flat 3	0.00	—	0.00	—	0.0	—
Media saturation							
4mCC 7	4mCC 8	0.00	—	0.00	—	0.0	—
4mCC 2	4mCC 7	0.22	4×5	2.48	4.5×5	2.7	$P_{20}(7,8)$
4mCC 1-ad	4mCC 2	3.92	4×6	4.13	4×6	8.1	$P_{20}(7-9)$
4mCC 3	4mCC 4	5.47	5.5×7	5.49	5.5×7	11.0	$P_{20}(7-10)$
4mCC 5-ad	4mCC 6-ad	7.37	5×7	7.21	5×7	14.6	$P_{20}(7-11)$
4mCC 1-bd	4mCC 2	5.63	4×6	5.90	4×6	11.5	$P_{20}(8-11)$
4mCC 5-bd	4mCC 6-bd	9.93	6×10	9.93	6×10	19.9	$P_{20}(8-11)$

^abd—before degradation, ad—after degradation.

Table 3 Supersonic laser, CSS He injection at 4.4 and 4.8 Torr, overtone outcoupled power, and beam size data as a function of mode volume and medium saturation; all of the mirrors are nominally 99.7% reflective except for the 4mCC nos. 7 and 8 mirrors, which are 98% reflective

Mirror no. 1 ^a	Mirror no. 2 ^a	CSS He injection, 4.4 Torr			CSS He injection, 4.8 Torr		
		Outcoupled power, W	Beam size, mm ²	Spectral lines lasing	Outcoupled power, W	Beam size, mm ²	Spectral lines lasing
Mode volume							
4mCC 5-ad	4mCC 6-ad	14.1	5×10	$P_{20}(7-10)$	10.4	5×10	$P_{20}(7-10)$
4mCC 1-ad	Flat 2	9.9	5×10	$P_{20}(7-11)$	7.3	4.5×8	$P_{20}(8-11)$
8mCC 1	8mCC 2	14.2	4×8	$P_{20}(7-11)$	10.1	4×8	$P_{20}(7-11)$
30mCC 1	30mCC 2	12.4	5×6.5	$P_{20}(7-11)$	7.4	4×7	$P_{20}(7-11)$
30mCC 2	Flat 2	12.7	4.5×5.5	$P_{20}(7-12)$	6.9	5×5	$P_{20}(7-11)$
Flat 2	Flat 3	nm ^b	nm	nm	nm	nm	nm
Media saturation							
4mCC 7	4mCC 8	nm	nm	nm	nm	nm	nm
4mCC 2	4mCC 7	1.0	3×4	$P_{20}(6,7)$	0.0	—	—
4mCC 1-ad	4mCC 2	7.6	4.5×10	$P_{20}(7-10)$	5.3	5×7	$P_{20}(7-10)$
4mCC 3	4mCC 4	11.7	6×11	$P_{20}(7-10)$	8.5	5.5×9.5	$P_{20}(7-10)$
4mCC 5-ad	4mCC 6-ad	14.1	5×10	$P_{20}(7-10)$	10.4	5×10	$P_{20}(7-10)$

^aad—after degradation. ^bnm—not measured.

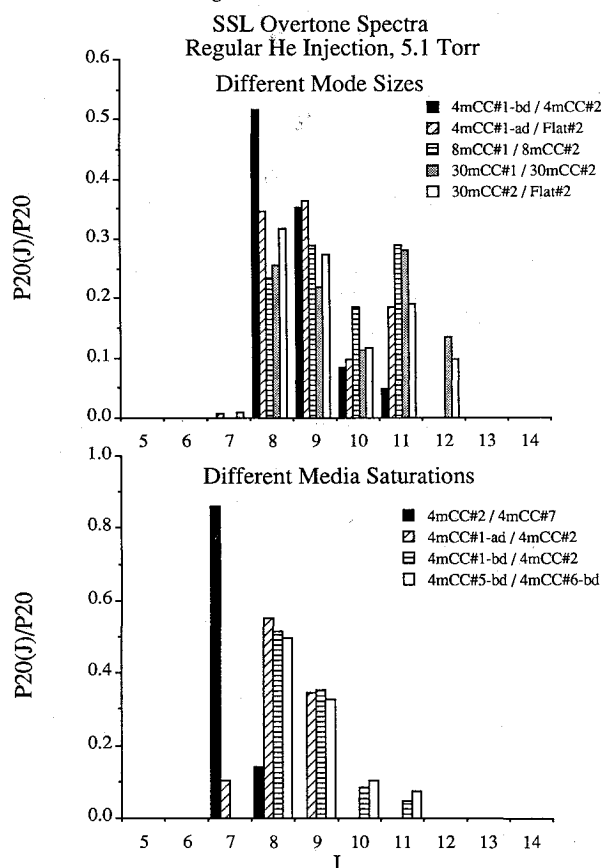


Fig. 2 Supersonic laser overtone spectra for different mode sizes and medium saturations for regular He injection at 5.1 Torr.

sively and now give a lower performance due to mirror degradation; they currently give 8 W of overtone power.

Figure 2 shows that different sets of 4mCC mirrors, which nominally all have the same reflectivity of 99.7% (4mCC 1-ad/2, 4mCC 1-bd/2, and 4mCC 5-bd/6-bd), yield different spectra. This illustrates the sensitivity of the low gain overtone system to variations in mirror reflectivity of less than 0.1%. However, for all three sets of 4mCC nominally 99.7% reflective mirrors, the primary lasing lines are $J=8$ and 9.

Lasing was not obtained, despite rigorous attempts, with two flats (nos. 2 and 3) or with the two 98% reflective 4mCC mirrors (4mCC nos. 7 and 8). Based on observations of extreme alignment sensitivity with the 30mCC/flat mirror combination, it is quite possible that vibrations transmitted to the optical bench from the vac-

uum pumps coupled with the low-gain overtone system were enough to prevent lasing with two flats.

From Refs. 11, 12, or 13, the optical beam waist as a function of mirror radii of curvature for a mirror separation of 1 m can be calculated for the fundamental and the overtone (the original resonator theory was worked out by Boyd and Gordon,¹⁴ and Boyd and Kogelnik¹⁵ for confocal resonators). The fundamental data were obtained with 2-m radii of curvature mirrors that give a zeroth-order optical beam waist of 1.75 mm. The 4-m, 8-m, and 30-m radii of curvature mirrors have overtone zeroth-order optical beam waists of 1.5, 1.75, and 2.50 mm, respectively. The data in Table 2 indicate that there was no significant change in overtone power or beam size as the mode volume (mirror radii of curvature) increased. However, a comparison of the spectra as the mode volume increased, Fig. 2, showed that there was an increase in the number of lasing lines and the spectra shifted toward higher J lines. There are several possibilities that may explain this observation. First, the larger radii of curvature mirrors might have a slightly higher reflectivity than the 4mCC mirrors. Second, the larger radii of curvature mirrors have a larger beam waist and hence sample the gain medium further downstream where the high J lines have larger gain than the lower J lines.

Although the observed beam width with the 8mCC and 30mCC mirrors was approximately the same as with the 4mCC mirrors, it was observed on the thermal image plate that, as the radii of curvature increased, the beam profile had fewer distinct modes lasing. From Refs. 11 and 12 it is clear that these distinct modal patterns were the result of lasing on a higher order transverse mode. Carter¹⁶ found an exact relation for the beam size at the $1/e$ dropoff point for the outermost intensity peak of a Hermite-Gaussian transverse mode of order m ; this equation related the zeroth-order mode size to the m th order mode size by a factor of $(2m+1)^{1/2}$. Chapter 4 of Ref. 11 provides useful forms of the relevant equations to compute the zeroth-order beam size for a symmetrical mirror resonator. Following the reasoning in Chap. 17 of Ref. 12, the modes that lase may have a beam size no greater than the size of a limiting aperture located within the resonator. Thus, there is a value m_{\max} that represents the highest order transverse mode that could lase for a given aperture inside the resonator. In the case of the UIUC SSL, the limiting aperture would be the gain zone itself because there are no restricting physical apertures other than the nozzle bank (where the gain zone begins). Calculations of m_{\max} for different mirror curvatures⁸ were in reasonable agreement with the observed transverse modal patterns.

A valley (minima) at $P_{20}(10)$ occurs in the spectra taken with all mirror combinations except pairs of 99.7% (or less) reflective 4mCC mirrors, see Fig. 2. This P_{20} minima is thought to be a consequence of a near resonant energy transfer¹⁷⁻¹⁹ from $v=3$ and $J=3,4$ to $v=2$ and $J=14$ with a subsequent rotational cascade to $v=2$ and $J=10, 11$, which are the upper levels for the $P_{20}(11)$ and $P_{20}(12)$ lines. Since $P_{20}(11)$ lases with the 8mCC/8mCC and

4mCC/flat mirror combinations and $P_{20}(11, 12)$ lase with the 30mCC/30mCC and 30mCC/flat mirror combinations, the rotational cascade to $v=2$ and $J=9$, which is the upper level for the $P_{20}(10)$ line, is blocked, resulting in $P_{20}(10)$ being weaker than $P_{20}(11)$ and $P_{20}(12)$.

The effect of medium saturation on overtone performance is illustrated in Table 2 and Fig. 2. Since the coatings of the nos. 1 and 2 4mCC mirrors degraded with use over a period of eight months, the original performance of these mirrors is also included in Table 2 together with the peak performance obtained from the nos. 5 and 6 4mCC mirrors. Figure 2 shows that, as the reflectivity of the mirrors increased from 98.0/99.7% (4mCC nos. 2/7) to approximately 99.68/99.67% (4mCC nos. 1/2 after degradation) to 99.78/99.67% (4mCC nos. 1/2 before degradation) to approximately 99.75/99.75% (4mCC nos. 5/6 before degradation), the outcoupled power increased and the spectra shifted toward higher J lines. These are the same trends observed for fundamental lasing. It is clear from Table 2 that a greater overtone power was obtained when the medium was driven harder, i.e., the 99.7/98% (4mCC nos. 2 and 7) mirrors gave a much lower power than any of the 99.7/99.7% combinations. No power was obtained when a lower medium saturation with two 98% mirrors (4mCC nos. 7 and 8) was tried.

Overtone performance data as a function of mode size and medium saturation for CSS He injection at 4.4 and 4.8 Torr are summarized in Table 3. The effects of increased medium saturation and mode size on outcoupled power and spectra (not shown) are qualitatively the same as observed for regular He injection. Overtone performance was sensitive to increased cavity pressure; significant amounts of power were lost when the pressure was increased by 0.4 Torr (see Table 3). Comparison of regular He injection overtone data (Table 2) with CSS injection overtone data (Table 3) shows comparable performance for both methods of He injection.

Significant beam diameter differences were observed between the two methods of He injection (Tables 2 and 3). CSS injection had beam diameters up to 11 mm for the 4mCC mirrors, which decreased as the mode volume increased, whereas regular He injection had typical beam diameters of 7 mm that decreased only slightly in size as the mode volume increased. The larger beam diameters exhibited by CSS data can be explained by the fact that longer 2→1 gain zones were measured⁹ (and most likely the 2→0 gain zones are also longer) for CSS injection than for regular He injection. One possible explanation for the observed decrease in CSS beam diameters is that the highest order modes that are capa-

ble of lasing still may have enough loss to favor lasing on a lower order mode. Therefore, even if an $m=21$ mode could lase, it is more likely that a lower order mode, say $m=18$, would lase because its loss would be significantly less. For the 4mCC mirrors the ratio of the $m=18$ beam size to the $m=21$ beam size is $[2(18)+1]^{1/2}/[2(21)+1]^{1/2}=0.93$, i.e., only a 7% difference. However, the highest order mode that could possibly lase with two 30mCC mirrors is $m=7$. It is then likely that the losses could be high enough to favor lasing on a lower order mode, say $m=4$. If this occurs, the beam size would be reduced by a factor of as much as $[2(4)+1]^{1/2}/[2(7)+1]^{1/2}=0.77$, a 23% decrease. The observed 11-mm beam diameter with the 4mCC mirrors could be reduced to 8.5 mm with the 30mCC mirrors; experimentally, the beam diameter of the 30mCC mirrors was measured as 7 mm. Thus, it seems plausible that the 4mCC mirrors with a large value for m_{\max} would be less affected by lasing on a mode a few integers less than m_{\max} than would the 30mCC mirrors. Therefore it is not unreasonable to observe significantly smaller beam diameters with the 30mCC mirrors than with the 4mCC mirrors for CSS injection. This effect was not as pronounced for regular He injection because the regular He injection gain zone was shorter than the CSS gain zone, thus restricting the size of the regular He injection beams.

IV. Overtone Efficiency

The overtone efficiency is defined to be the ratio of the overtone power to the maximum total fundamental power,

$$\phi = \frac{P_{\text{Overtone}}}{(P_{\text{Fundamental}})_{\text{Max}}} \quad (1)$$

Since the overtone mirrors have large inferred absorption plus scattering ($A+S$) losses (Table 1), the measured outcoupled overtone power will be less than the total outcoupled overtone power. Thus, to estimate the overtone efficiency, the total overtone power must be estimated. The total overtone power is

$$P_{\text{total}} = P_{\text{out}} + P_{\text{AS}} \quad (2)$$

where P_{total} is the total overtone power, P_{out} is the measured outcoupled power, and P_{AS} is the power lost to mirror absorption and scattering. The absorbed/scattered power is calculated from the inferred absorption/scattering loss (Table 1) and the intracavity power

$$P_{\text{AS}} = P_{\text{IC}}(AS_1 + AS_2) \quad (3)$$

Table 4 Estimates of the absorption/scattering losses and the overtone efficiency as a function of mode volume and medium saturation for regular He injection at 5.1 Torr; overtone efficiency is calculated by dividing the total overtone power by the maximum fundamental power of 63.0–76.2 W.

Mirror no. 1 ^a	Mirror no. 2 ^a	PIC: based on UIUC transmissivity measurements, W	Outcoupled power, W	Absorbed/ scattered power, W	Total power, W	Estimated overtone efficiency, %
Mode volume						
4mCC 1-ad	4mCC 2	6183	8.1	32.1	40.2	52.9–63.8
4mCC 1-ad	Flat 2	8963	12.1	43.5	55.6	73.1–88.3
8mCC 1	8mCC 2	7256	11.9	31.6	43.5	57.1–69.0
30mCC 1	30mCC 2	7654	12.4	33.5	45.9	60.2–72.9
30mCC 2	Flat 2	8389	12.5	37.8	50.3	66.0–79.8
Flat 2	Flat 3	—	—	—	—	—
Media saturation						
4mCC 7	4mCC 8	—	—	—	—	—
4mCC 2	4mCC 7	226	2.7	2.5	5.2	6.8–8.3
4mCC 1-ad	4mCC 2	6183	8.1	32.1	40.2	52.9–63.8
4mCC 3	4mCC 4	7190	11.0	32.1	43.1	56.6–68.4
4mCC 5-ad	4mCC 6-ad	9419	14.6	41.9	56.5	74.1–89.7
4mCC 1-bd	4mCC 2	10,454	11.5	46.0	57.5	75.5–91.3
4mCC 5-bd	4mCC 6-bd	12,839	19.9	44.3	64.2	84.3–101.9

^aad—after degradation, bd—before degradation.

Table 5 Estimates of the absorption/scattering losses and the overtone efficiency as a function of mode volume and medium saturation for CSS He injection at 4.4 and 4.8 Torr; overtone efficiency is calculated by dividing the total overtone power by the maximum fundamental power of 58.5–70.8 W at 4.4 Torr and 51.7–62.6 W at 4.8 Torr

		CSS He injection, 4.4 Torr			CSS He injection, 4.8 Torr		
Mirror no. 1 ^a	Mirror no. 2 ^a	Outcoupled power, W	Total power, W	Estimated overtone efficiency, %	Outcoupled power, W	Total power, W	Estimated overtone efficiency, %
Mode volume							
4mCC 5-ad	4mCC 6-ad	14.1	54.6	77.1–93.3	10.4	40.3	64.4–77.9
4mCC 1-ad	Flat 2	9.9	45.5	64.3–77.8	7.3	30.8	49.2–59.6
8mCC 1	8mCC 2	14.2	52.0	73.4–88.9	10.1	37.0	59.1–71.6
30mCC 1	30mCC 2	12.4	39.3	55.5–67.2	7.4	27.4	43.8–53.0
30mCC 2	Flat 2	12.7	51.1	72.2–87.3	6.9	27.8	44.4–53.8
Flat 2	Flat 3	nm ^b	nm	nm	nm	nm	nm
Media saturation							
4mCC 7	4mCC 8	nm	nm	nm	nm	nm	nm
4mCC 2	4mCC 7	1.0	1.9	2.7–3.2	0.0	0.0	0.0
4mCC 1-ad	4mCC 2	7.6	37.7	53.2–64.4	5.3	26.3	42.0–50.9
4mCC 3	4mCC 4	11.7	45.9	64.8–78.5	8.5	33.3	53.2–64.4
4mCC 5-ad	4mCC 6-ad	14.1	54.6	77.1–93.3	10.4	40.3	64.4–77.9

^aad—after degradation, bd—before degradation. ^bnm—not measured.

where P_{IC} is the intracavity power and AS_x is the inferred absorption/scattering loss of mirror x (Table 1). The intracavity power is given by

$$P_{IC} = \frac{P_{out}}{T_1 + T_2} \quad (4)$$

where T_1 and T_2 are the transmissivities of the two mirrors. Substitution of Eqs. (3) and (4) into Eq. (2) gives

$$P_{total} = P_{out} \left(1 + \frac{AS_1 + AS_2}{T_1 + T_2} \right) \quad (5)$$

for the total overtone power, Table 1 shows that the 99.7% reflective mirrors have an inferred absorption/scattering loss that is typically two to four times larger than the transmitted percentage. Thus, for example, Eq. (5) gives that the 4mCC nos. 1 and 2 mirrors (before degradation) have a P_{total} equal to 4.2 ($=1+3.2$) times the outcoupled overtone power, i.e., the absorbed/scattered power is 76% ($=3.2/4.2$) of the total available overtone power. Jeffers¹ measured overtone scattering losses that ranged from 10–64% of the total observed overtone power, where the total power consists of transmitted, absorbed, and scattered powers measured calorimetrically. Because of experimental limitations that prevented all of the scattered power from being measured, Jeffers estimated that 17–78% of the total overtone power was actually lost to scattering. Thus, a 76% scattering loss is not unreasonable.

A. Overtone Efficiency of the UIUC Supersonic Laser

Using Eqs. (1–5) and Tables 1–3, the intracavity power, absorbed/scattered power, total overtone power, and overtone efficiency of the UIUC SSL were estimated as a function of medium saturation, mode volume (mirror radius of curvature), cavity pressure, and method of He injection (Tables 4 and 5). The overtone efficiencies for regular He injection were calculated by dividing the total overtone power by the maximum fundamental power of 63.0–76.2 W at 5.1 Torr. The overtone efficiencies for CSS He injection were calculated by dividing the total overtone power by the maximum fundamental power of 58.5–70.8 W at 4.4 Torr and by the maximum fundamental power of 51.7–62.6 W at 4.8 Torr (Sec. II.B).

The most important point from Tables 4 and 5 is that overtone efficiencies of 70–90% have been obtained experimentally. These are the highest overtone efficiencies reported to date.⁵ Overtone efficiencies of 70–90% are in good agreement with theoretical maximum efficiency estimates of 50–80%.^{3,20}

With the estimates of the overtone efficiencies for the different sets of overtone mirrors, the effects of mode volume and medium

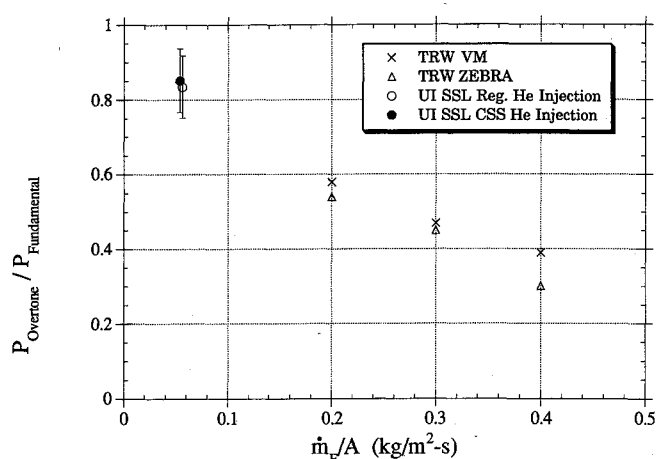


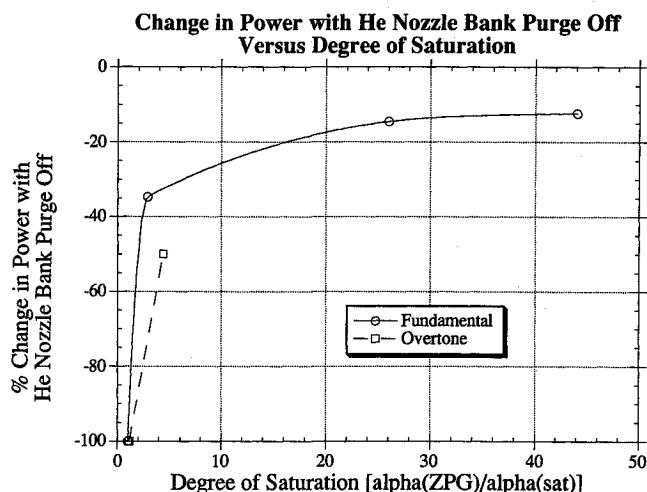
Fig. 3 Overtone efficiency as a function of \dot{m}_F/A for different HF chemical lasers.

saturation on overtone performance can be examined. The data in Table 4 indicate that there is no significant change in overtone efficiency as the mode volume (mirror radii of curvature) increased. It is clear from Table 4 that a greater overtone efficiency is obtained when the medium is driven harder, i.e., the 99.7/98% (4mCC nos. 2 and 7) mirror combination gave a much lower efficiency than any of the 99.7/99.7% combinations. In fact, all of these 99.7/99.7% combinations gave about the same efficiency. The CSS data show similar trends (Table 5).

A comparison of the CSS He injection data in Table 5 with the regular He injection data in Table 4 shows that the overtone efficiencies obtained with the same set of mirrors (nominally 99.7/99.7%) are approximately the same independent of the method of He injection. Thus, it is possible to extract 70–90% of the fundamental power in the overtone for both methods of He injection for our supersonic laser. However, there was an average decrease of 16% in overtone efficiency for the 4.8 Torr CSS injection data compared with the 4.4 Torr overtone efficiencies. This indicates that pressure has an effect on CSS overtone efficiency in contrast to regular He injection results, which showed no pressure effect on overtone efficiency.⁸ For CSS injection, the peak overtone efficiency was 93% at 4.4 Torr and 78% at 4.8 Torr; for regular He injection, the peak efficiency was 90%. In all three cases the peak efficiency occurred with the same two 4mCC mirrors (nos. 5 and 6). This suggests that, for a device optimized for fundamental performance, overtone efficiencies of 70–90% may be obtainable regardless of the device used.

Table 6 Fundamental and overtone SSL power and spectral data for different mirrors (different medium saturations) when the He nozzle bank purge (base absorption purge) is on or off

Mirror reflectivity, %/%	Max. α_{ZPG} , 1/cm	α_{sat} , 1/cm	Degree of saturation, $\alpha_{ZPG}/\alpha_{sat}$	He nozzle bank purge	Power, W	Change in power, %	Spectra	P_{10}/P_{Tot}
Fundamental								
50/99.5	0.1144	0.03957	2.89	On	37.6		$P_1(6-9), P_2(6-9)$	0.598
				Off	24.6	-34.6	$P_1(7,8), P_2(6-9)$	0.561
93/99.5	0.1144	0.004397	26.02	On	58.0		$P_1(8-13), P_2(8-13)$	0.541
				Off	49.6	-14.5	$P_1(8-13), P_2(8-13)$	0.501
96/99.5	0.1144	0.002598	44.05	On	63.2		$P_1(8-15), P_2(8-13)$	0.500
				Off	55.4	-12.3	$P_1(8-15), P_2(8-13)$	0.441
Overtone								
98.0/99.7	0.001498	0.001315	1.14	On	5.2		$P_{20}(6-8)$	na
				Off	0.0	-100.0	None	na
99.7/99.7	0.001498	0.0003406	4.40	On	10.2		$P_{20}(7-9)$	na
				Off	5.1	-50.0	$P_{20}(8-10)$	na

**Fig. 4** Percent reduction in total fundamental and overtone powers as a function of the degree of saturation when the He base region purge was turned off.

The UIUC SSL overtone data presented earlier can be compared with TRW VM and ZEBRA data.⁵ Blaze II²¹ and ORNECL²⁰ modeling studies for the SSL gave 7% SF₆ dissociation for regular He injection and 12.5% for CSS injection. Using these SF₆ dissociation percentages, the mass flow rate of fluorine atoms was computed. The UIUC SSL overtone efficiencies are compared with the TRW data as a function of \dot{m}_F/A (Fig. 3). From this figure, it is seen that the UIUC SSL data fall on a straight line extrapolation of the TRW data.

The obvious question that arises from Fig. 3 is, why does \dot{m}_F/A influence overtone efficiency? There are two significant differences between the HF chemical lasers compared in Fig. 3. First, the TRW lasers, VM and ZEBRA, have significantly different mixing characteristics than the UIUC supersonic laser. Second, the TRW lasers are both combustor-driven devices; these devices have ground state deuterium-fluoride (DF) in the primary stream (DF is a byproduct of the NF₃-D₂ reaction to obtain free F atoms). The UIUC supersonic laser is an arc-driven device that does not have DF in its flow. The effects of different mixing schemes and DF on overtone performance are the subject of current studies.

B. Effects of Purging Base Absorption Region

To investigate the effects of the He nozzle bank purge as a function of reflectivity and wavelength, fundamental and overtone power and spectra were measured for several mirror combinations to vary the saturation level in the laser (Table 6). The degree of saturation in the laser is indicated by the ratio of the maximum zero power gain (ZPG) to the saturated gain α_{sat} for the given mirror combination. Since overtone ZPG data are not available and it was desired to compare the fundamental and the overtone results, the

maximum ZPGs calculated by the ORNECL computer model²⁰ were used for both the fundamental and the overtone. The maximum fundamental ZPG of 0.1144 cm⁻¹ occurred on line P₂(6) 1.3 mm downstream from the nozzle exit plane. The maximum overtone ZPG of 0.001498 cm⁻¹ occurred on line P₂₀(7) at the same location. At this location in the cavity, the Blaze II computer code²¹ computes the gain length L_e as 8.82 cm; the saturated gain is given by

$$\alpha_{sat} = -\frac{1}{2L_e} \ln(r_1 r_2) \quad (6)$$

where r_1 and r_2 are the reflectivities of the two mirrors. The degree of saturation for regular He injection at 5.1 Torr is 2.1, 2.9, 4.3, 6.3, 26.0, and 44.1 for the 38, 50, 63, 73, 93, and 96% reflective fundamental outcouplers, respectively (a 99.5% reflector was used in combination with the aforementioned fundamental outcouplers). The degree of saturation for regular He injection at 5.1 Torr is 1.1 and 4.4 for the 98.0/99.7% and 99.7/99.7% reflective overtone mirror combinations, respectively. The degree of saturation in the overtone with two 99.7% overtone mirrors is approximately the same as in the 63% fundamental case.

Figure 4 shows the percent change in power when the nozzle bank He base purge was turned off vs the degree of saturation. The data shown in Fig. 4 clearly illustrate that HF(0) absorption in the base region became less important as the degree of saturation increased; however, the curve levels off and indicates that approximately 10% of the available fundamental power will be lost even at very high saturations. The overtone data suggest that the overtone performance is more sensitive to base region absorption due to HF(0). This is reasonable since the fundamental 2→1 lasing is not directly affected by HF(0), whereas the fundamental 1→0 and the overtone 2→0 transitions are directly affected by the presence of ground state HF. This statement is supported by fundamental data in Table 6 that show that the power split between vibrational bands, P_{10}/P_{Tot} , decreased when the He nozzle bank purge was turned off, i.e., base ground state HF absorption reduced 1→0 lasing more than 2→1 lasing.

These results suggest the following conclusions. First, base region absorption becomes less important as the degree of saturation increases for both fundamental and overtone wavelengths. Second, overtone performance is more sensitive to purging of base region HF(0) than is fundamental performance because the overtone transitions are directly linked to ground state HF populations. Third, because the overtone zero power gains are significantly lower than those of the fundamental, it is much harder to obtain the same degree of saturation in the overtone; consequently, it may be much harder to reach saturation levels where the base region absorption has only a 10% effect on overtone power.

V. Concluding Remarks

The various parameters studied that affect overtone performance were medium saturation, mode volume, cavity pressure, base

region absorption, gas flow rates, and the method of He injection. Experimental factors that were vital to good overtone performance were good mirror alignment, clean mirrors, and the elimination of the loss produced by intracavity Brewster windows.

The most significant parameter affecting overtone performance and efficiency was medium saturation. When the medium was well saturated (degree of saturation was increased to 4.4), overtone efficiencies of 70–90% were observed. These are the highest overtone efficiencies reported to date.⁵ Overtone efficiencies of 70–90% are in good agreement with theoretical maximum efficiency estimates of 50–80%.^{3,20} However, when the degree of saturation (the ratio of maximum zero power gain to saturated gain) was near unity, overtone efficiencies of about 10% were observed.

Overtone efficiency was insensitive to changes in mode volume. Smaller mode sizes (obtained using smaller radii of curvature mirrors) produced higher order transverse mode patterns but also decreased the alignment and laser stability problems encountered with larger radii of curvature mirrors.

The gas flow rates that optimized the fundamental performance of the UIUC SSL also optimized the overtone performance of the laser.

Increased cavity pressure reduced both the total fundamental and overtone powers but did not significantly affect the overtone efficiency of the laser.

Base region absorption by ground state HF has a significant effect on overtone performance and efficiency. As the degree of saturation increased (mirror reflectivity increased), the percent reduction in power decreased when the He base region purge was turned off for both the fundamental and overtone wavelengths. However, even with very high degrees of saturation for the fundamental (20–50), approximately 10% of the total power was lost when the He purge was turned off. Since the overtone zero power gains are about two orders of magnitude less than the fundamental zero power gains, it is much harder to obtain the same degree of saturation in the overtone as in the fundamental. Hence, with the highest overtone degrees of saturation obtainable (4–5), approximately 50% of the overtone power was lost when the He base region purge was turned off. Thus, proper purging of base absorption regions is essential for good overtone performance.

The method of He injection did not significantly influence the overtone efficiency of the UIUC SSL. This suggests the possibility that overtone efficiencies of 70–90% may be obtainable regardless of the device used so long as the aforementioned parameters and experimental conditions are properly handled, i.e., high degree of saturation, proper base region purging, optimized gas flow rates, the use of clean (uncontaminated) overtone mirrors, and the removal of extraneous intracavity losses such as Brewster windows.

Acknowledgment

This work was supported by the Strategic Defense Initiative Organization through W. J. Schafer Associates subcontract SC-88K-33-004.

References

¹Jeffers, W. Q., "Short Wavelength Chemical Laser Technology Development," Helios, Inc., Longmont, CO, Final Report for Directed

Energy Directorate, Research, Development, and Engineering Center, U.S. Army Missile Command, Redstone Arsenal, AL, Oct. 1988.

²Jeffers, W. Q., "Short Wavelength Chemical Lasers," *AIAA Journal*, Vol. 27, No. 1, 1989, pp. 64–66.

³Smith, W., Howie, S. S., Long, J., Taylor, S., and Acebal, R., "HF Overtone Laser Device Performance Modeling and Data Correlation," Science Applications International Corp., DAAH01-86-D-0007, Marietta, GA, May 1989.

⁴Duncan, W., Holloman, M., Rogers, B., and Patterson, S., "Hydrogen Fluoride Overtone Chemical Laser Technology," AIAA Paper 89-1903, June 1989.

⁵Duncan, W., Patterson, S., Graves, B., and Holloman, M., "Recent Progress in Hydrogen Fluoride Overtone Chemical Lasers," AIAA Paper 91-1480, June 1991.

⁶Smith, W., and Schafer, E., "Gain Medium Considerations in the Design of Overtone Chemical Laser Resonators," AIAA Paper 91-1481, June 1991.

⁷Sentman, L. H., Theodoropoulos, P. T., Nguyen, T., Carroll, D., and Waldo, R., "An Economical Supersonic cw HF Laser Testbed," AIAA Paper 89-1898, June 1989.

⁸Carroll, D. L., Sentman, L. H., Theodoropoulos, P. T., Waldo, R. W., Gordon, S. J., and Otto, J. W., "Experimental and Theoretical Study of cw HF Chemical Laser Overtone Performance," Univ. of Illinois, TR 92-2, UILU Eng. 92-0502, Aeronautical and Astronautical Engineering Dept., Urbana, IL, March, 1992.

⁹Sentman, L. H., Nguyen, T. X., Theodoropoulos, P. T., Waldo, R. E., and Carroll, D. L., "An Experimental Study of Supersonic cw HF Chemical Laser Zero Power Gain," Univ. of Illinois, TR 89-6 UILU Eng. 89-0506, Aeronautical and Astronautical Engineering Dept., Urbana, IL, Aug. 1989.

¹⁰Herbelin, J. M., and McKay, J. A., "Development of Laser Mirrors of Very High Reflectivity Using the Cavity-Attenuated Phase-Shift Method," *Applied Optics*, Vol. 20, No. 9, 1981, pp. 3341–3344.

¹¹Yariv, A., *Optical Electronics*, Holt, Rinehart and Winston, New York, 1985.

¹²Siegman, A. E., *Lasers*, Univ. Science Books, Mill Valley, CA, 1986.

¹³Chodsko, R. A., and Chester, A. N., "Optical Aspects of Chemical Lasers," *Handbook of Chemical Lasers*, edited by R. W. F. Gross, and J. F. Bott, Wiley, New York, 1976, pp. 95–203.

¹⁴Boyd, G. D., and Gordon, J. P., "Confocal Multimode Resonator for Millimeter Through Optical Wavelength Masers," *Bell System Technical Journal*, Vol. 40, March 1961, pp. 489–507.

¹⁵Boyd, G. D., and Kogelnik, H., "Generalized Confocal Resonator Theory," *Bell System Technical Journal*, Vol. 41, July 1962, pp. 1347–1369.

¹⁶Carter, W. H., "Spot Size and Divergence for Hermite Gaussian Beams of Any Order," *Applied Optics*, Vol. 19, No. 7, April 1980, pp. 1027–1029.

¹⁷Sentman, L. H., Nayfeh, M. H., Renzoni, P., King, K., Townsend, S., and Tsioulos, G., "Saturation Effects in a cw HF Chemical Laser," *AIAA Journal*, Vol. 23, No. 9, 1985, pp. 1392–1401.

¹⁸Sentman, L. H., Tsioulos, G., Bichanich, J., and Carroll, D. L., "An Experimental Study of Fabry-Perot and Stable Resonator cw HF Chemical Laser Performance," Univ. of Illinois, TR 85-3, UILU Eng. 85-0503, Aeronautical and Astronautical Engineering Dept., Urbana, IL, March 1985.

¹⁹Sentman, L. H., Carroll, D. L., Theodoropoulos, P., and Gumus, A., "Scale Effects in a cw HF Chemical Laser," Univ. of Illinois, TR 86-5, UILU Eng. 86-0505, Aeronautical and Astronautical Engineering Dept., Urbana, IL, Sept. 1986.

²⁰Sentman, L. H., Carroll, D. L., and Gilmore, J., "Modeling cw HF Fundamental and Overtone Lasers," AIAA Paper 89-1904, June 1989.

²¹Sentman, L. H., Subbiah, M., and Zelazny, S. W., "Blaze II: A Chemical Laser Simulation Computer Program," Bell Aerospace Textron, T.R. H-CR-77-8, Buffalo, NY, Feb. 1977.